

Supplementary Materials for

The Huntingtin-interacting protein SETD2/HYPB is an actin lysine methyltransferase

Riyad N. H. Seervai*, Rahul K. Jangid, Menuka Karki, Durga Nand Tripathi, Sung Yun Jung, Sarah E. Kearns, Kristen J. Verhey, Michael A. Cianfrocco, Bryan A. Millis, Matthew J. Tyska, Frank M. Mason, W. Kimryn Rathmell, In Young Park*, Ruhee Dere*, Cheryl Lyn Walker*

*Corresponding author. Email: riyad.seervai@bcm.edu (R.N.H.S.); cheryl.walker@bcm.edu (C.L.W.); ipark@bcm.edu (I.Y.P.); dere@bcm.edu (R.D.)

Published 2 October 2020, *Sci. Adv.* **6**, eabb7854 (2020)

DOI: 10.1126/sciadv.abb7854

The PDF file includes:

Figs. S1 to S10

Legends for movies S1 to S3

Other Supplementary Material for this manuscript includes the following:

(available at advances.sciencemag.org/cgi/content/full/6/40/eabb7854/DC1)

Movies S1 to S3

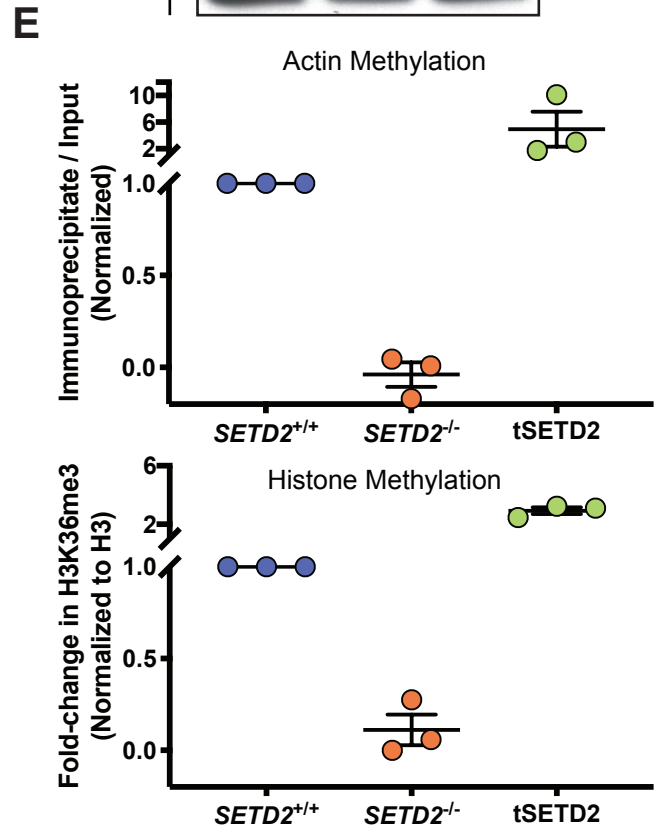
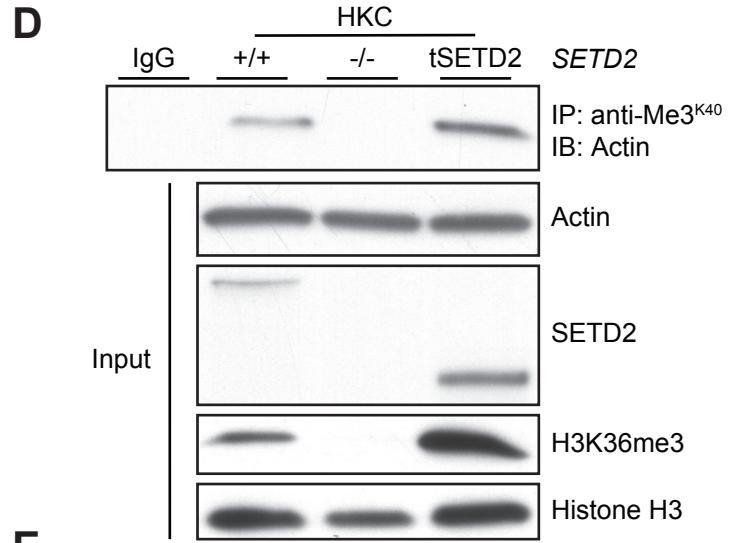
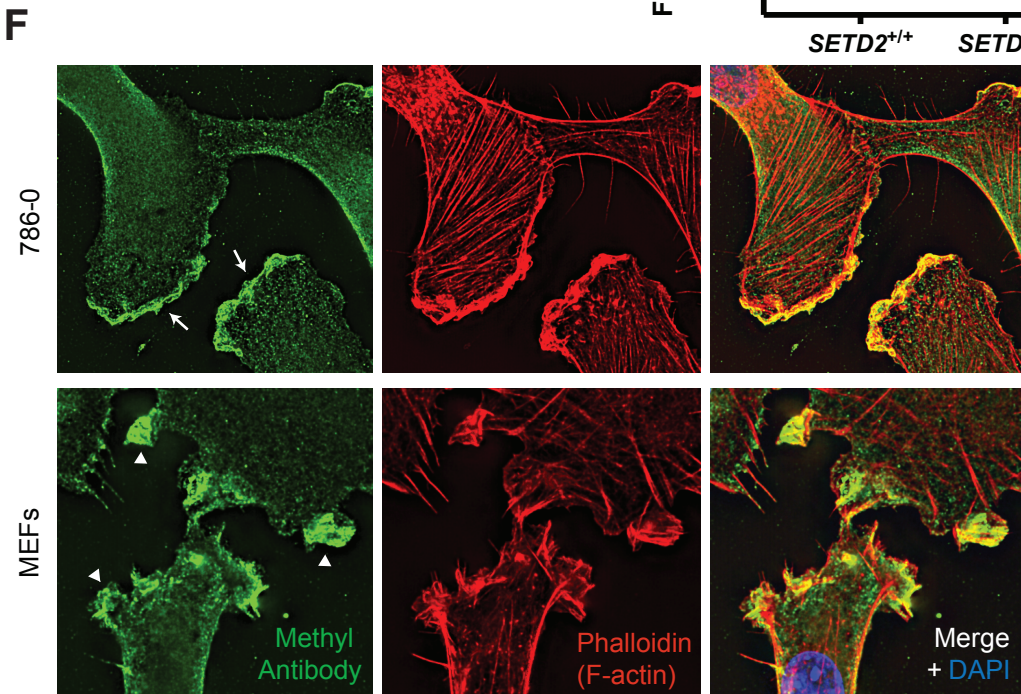
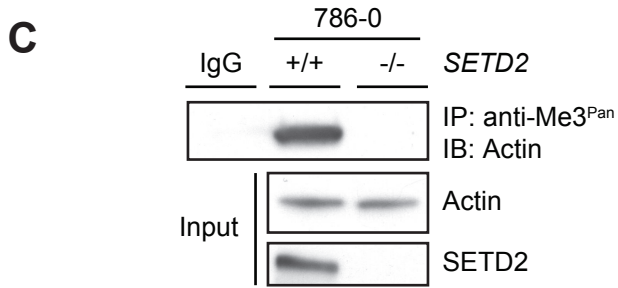
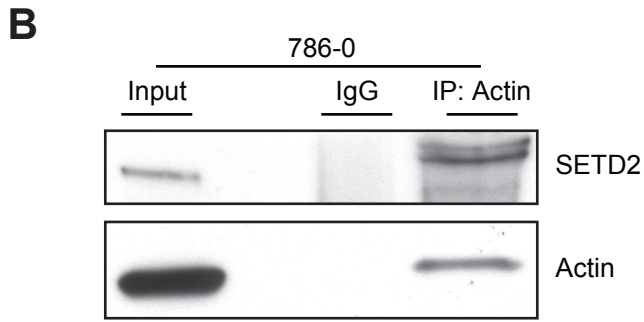
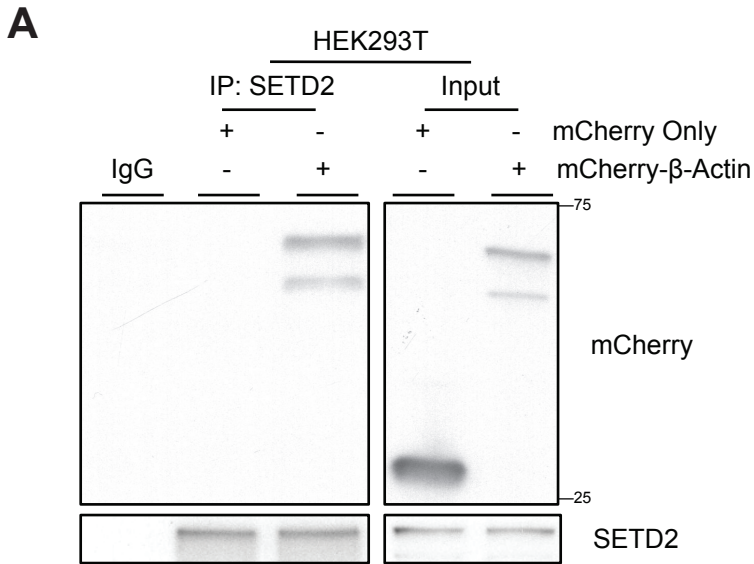
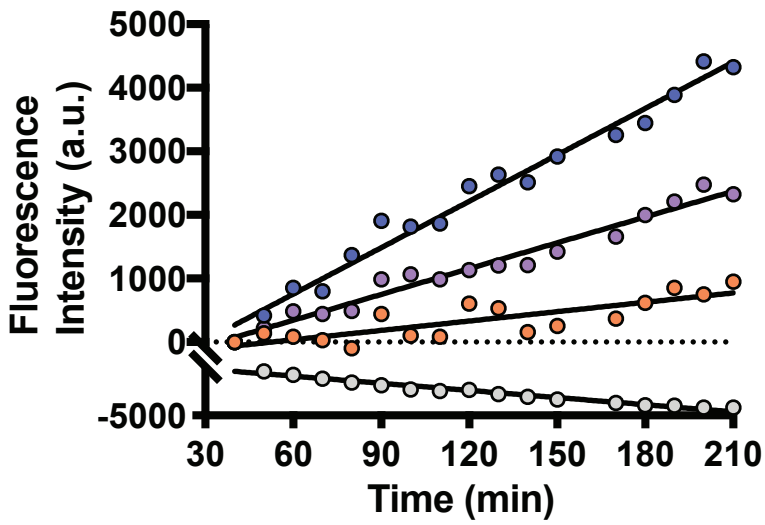


Figure S1. Interaction between SETD2 and actin. (A) Immunoblot analysis showing co-immunoprecipitation of endogenous SETD2 with mCherry- β -actin in HEK293T cells. (B) Co-immunoprecipitation of endogenous actin with endogenous SETD2 in 786-0 cells (reciprocal co-IP from data shown in in Fig. 1B). (C) Immunoprecipitation of actin from SETD2-proficient but not SETD2-deficient 786-0 cells using a pan-trimethyl lysine (anti-Me3^{Pan}) antibody. Data in (A) to (C) are representative of experiments repeated at least three times with similar results. (D and E) Immunoblot analysis (D) and quantitation (E) showing immunoprecipitation of actin using anti-Me3^{K40} SETD2 methyl-epitope antibody in SETD2-proficient but not SETD2-deficient HKC cells, and rescued by re-expression of truncated SETD2 (tSETD2). Presence or absence of the H3K36me3 histone methyl mark used as a control for SETD2 methyltransferase activity. Data are mean \pm S.E.M. for each biological replicate (n=3). (F) Deconvolution microscopy imaging of 786-0 and mouse embryonic fibroblast (MEF) cells showing localization of the SETD2 methyl epitope (green) to areas of high actin turnover, including ruffles (white arrowheads) and lamellipodia (white arrows) at the leading edge of cells. F-actin stained using phalloidin (shown in red).

A

- rActin (HEK293T)
- Skeletal Muscle
- rActin (*E.coli*)
- Actins Only

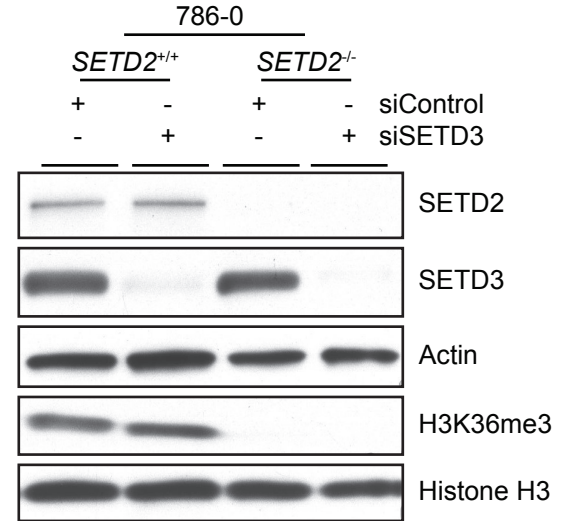
B**C**

Figure S2. SETD2 methylation of actin. (A) Fluorescence-based quantitation of *in vitro* methylation using GST-tagged SETD2 catalytic SET domain (a.a. 1418-1714) with purified skeletal muscle actin (purple), and recombinant actin (rActin) from HEK293T cells (blue) or *E. coli* (orange). Actin proteins alone (grey) shown as negative control. Fluorescence signal calculated after subtracting automethylation from samples with SETD2 alone. (B) Immunoblot analysis showing expression of SETD3 in both parental and SETD2-deficient 786-0 cells, with *SETD3* knockdown used to demonstrate specificity for this antibody. (C) Immunoprecipitation of actin from control and *SETD3* knockdown 786-0 cells using SETD2 methyl-epitope antibody (anti-Me3^{K36}). The input blot showing SETD3 expression is a section of the blot shown in (C). Data are representative of experiments repeated at least three times with similar results.

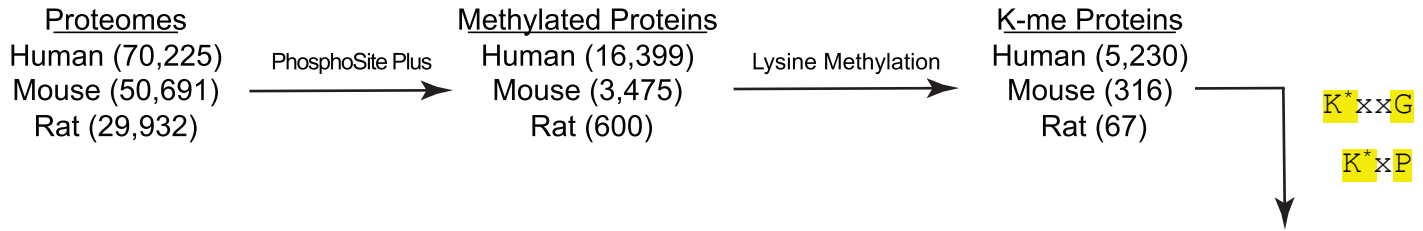
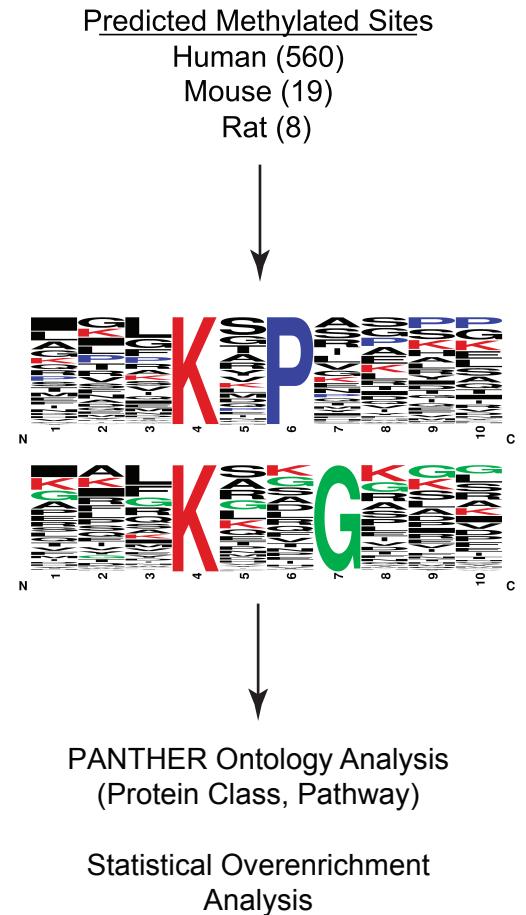
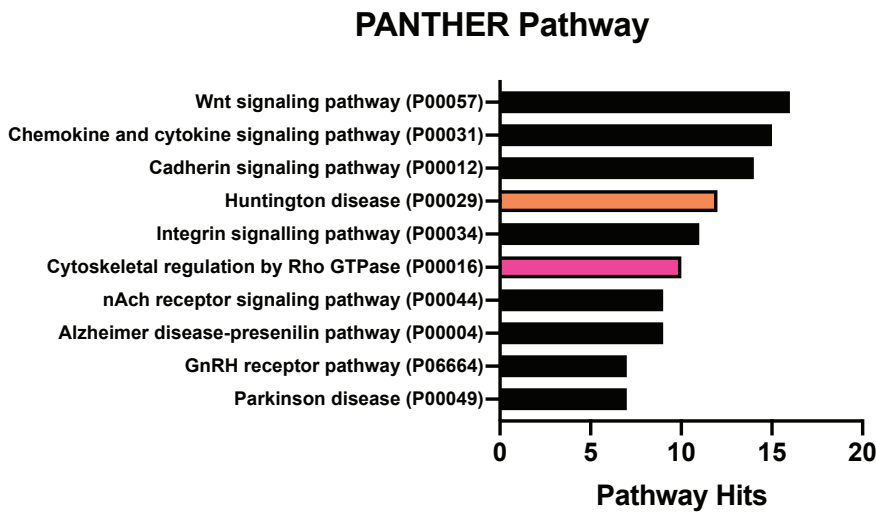
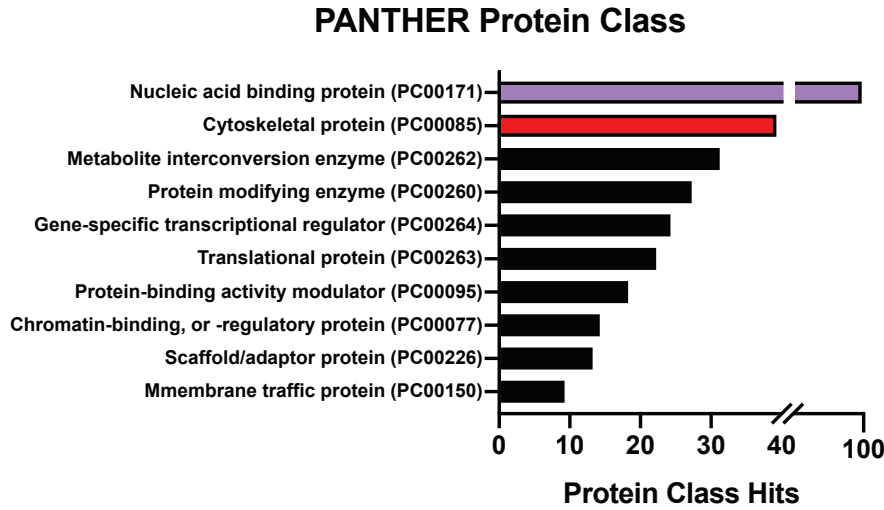
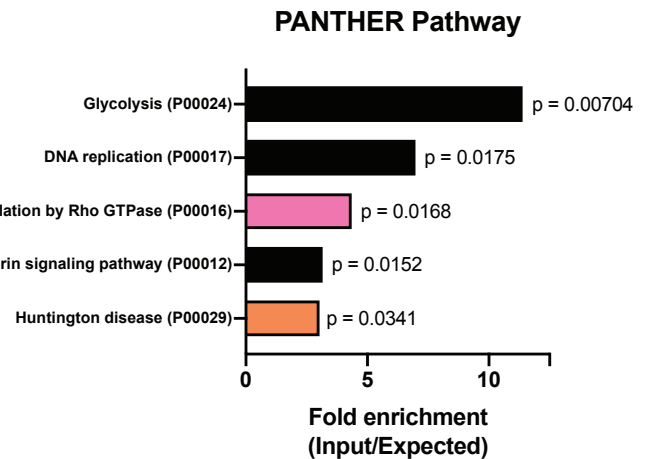
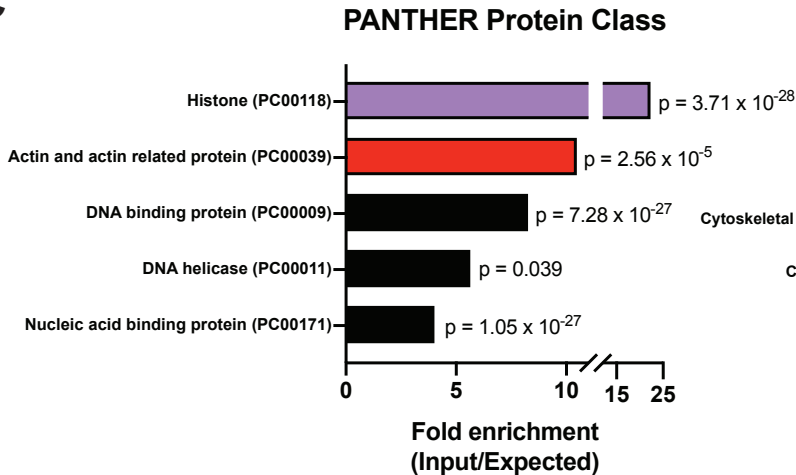
A**B****C**

Figure S3. Identification of SETD2 methylation site on actin. (A) Schematic for pipeline identifying proteins with lysine methylation at known SETD2 recognition motif sites, using methylation site data downloaded from PhosphoSitePlus®. Amino acid sequences for KxP- and KxxG- containing proteins generated using weblogo.berkeley.edu. (B) Ontology analysis showing the top 10 protein classes (top) and pathways (bottom) with proteins identified in (A) found to be methylated at a SETD2 recognition motif. (C) Overrepresentation analysis showing the top 5 protein classes (left) and pathways (right) from analysis shown in (A). Protein classes and pathways of interest in (B) and (C) are highlighted in color.

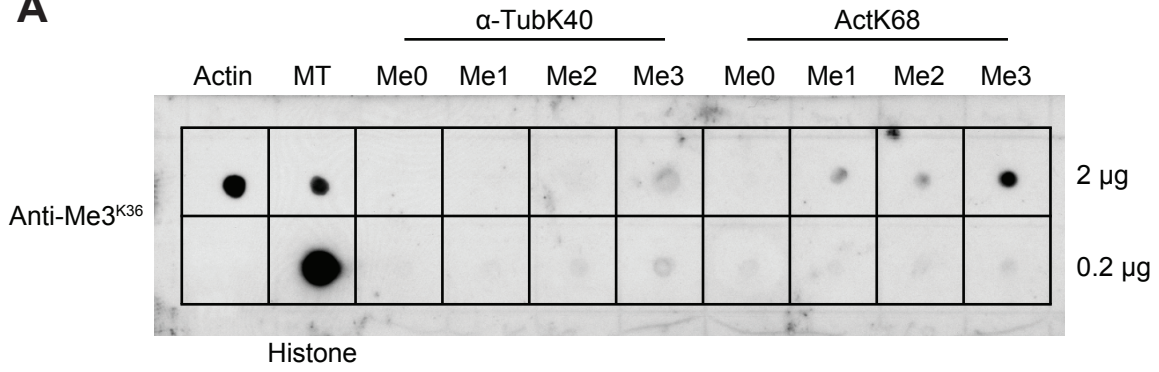
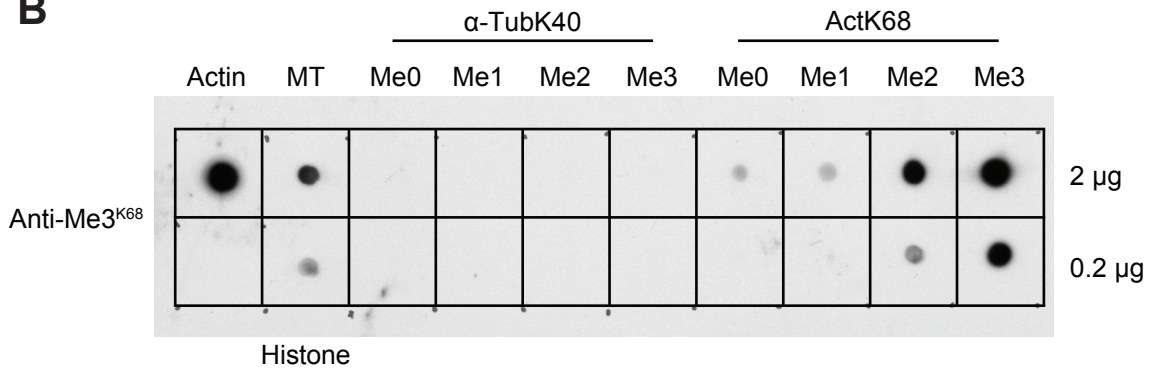
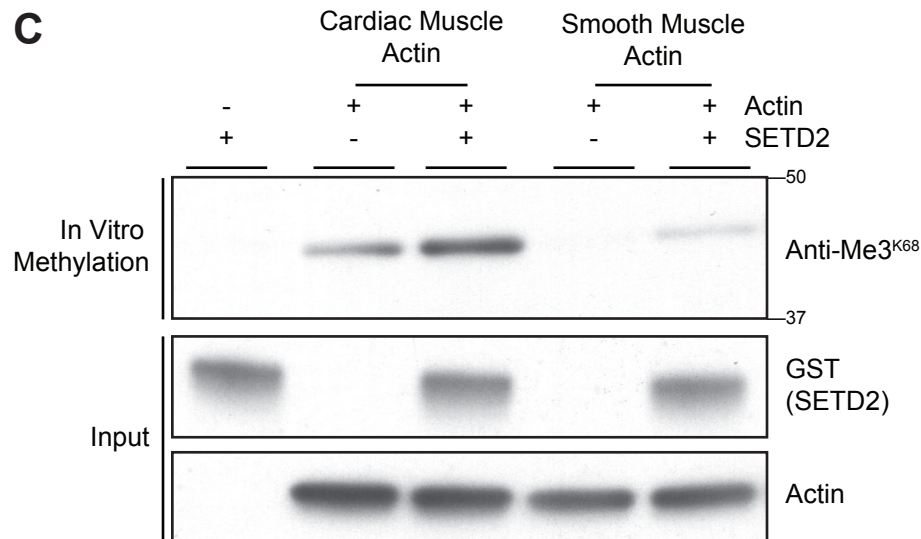
A**B****C**

Figure S4. Characterization of ActK68 methylation site. (A and B) Dot blot showing specificity of anti-Me3^{K36} (A) and anti-Me3^{K68} (B) antibodies. Methylated tubulin peptides, as well as purified muscle actin, microtubules (MT), and histone proteins also shown. The anti-Me3^{K36} antibody shows cross-reactivity with trimethylated ActK68 peptides. The anti-Me3^{K68} antibody shows little cross-reactivity with purified histones/nucleosomes. (C) Immunoblot analysis showing recognition of actin proteins by anti-Me3^{K68} antibody following *in vitro* methylation with GST-tagged SETD2 (a.a. 1418-1714). Data are representative of experiments repeated at least three times with similar results.

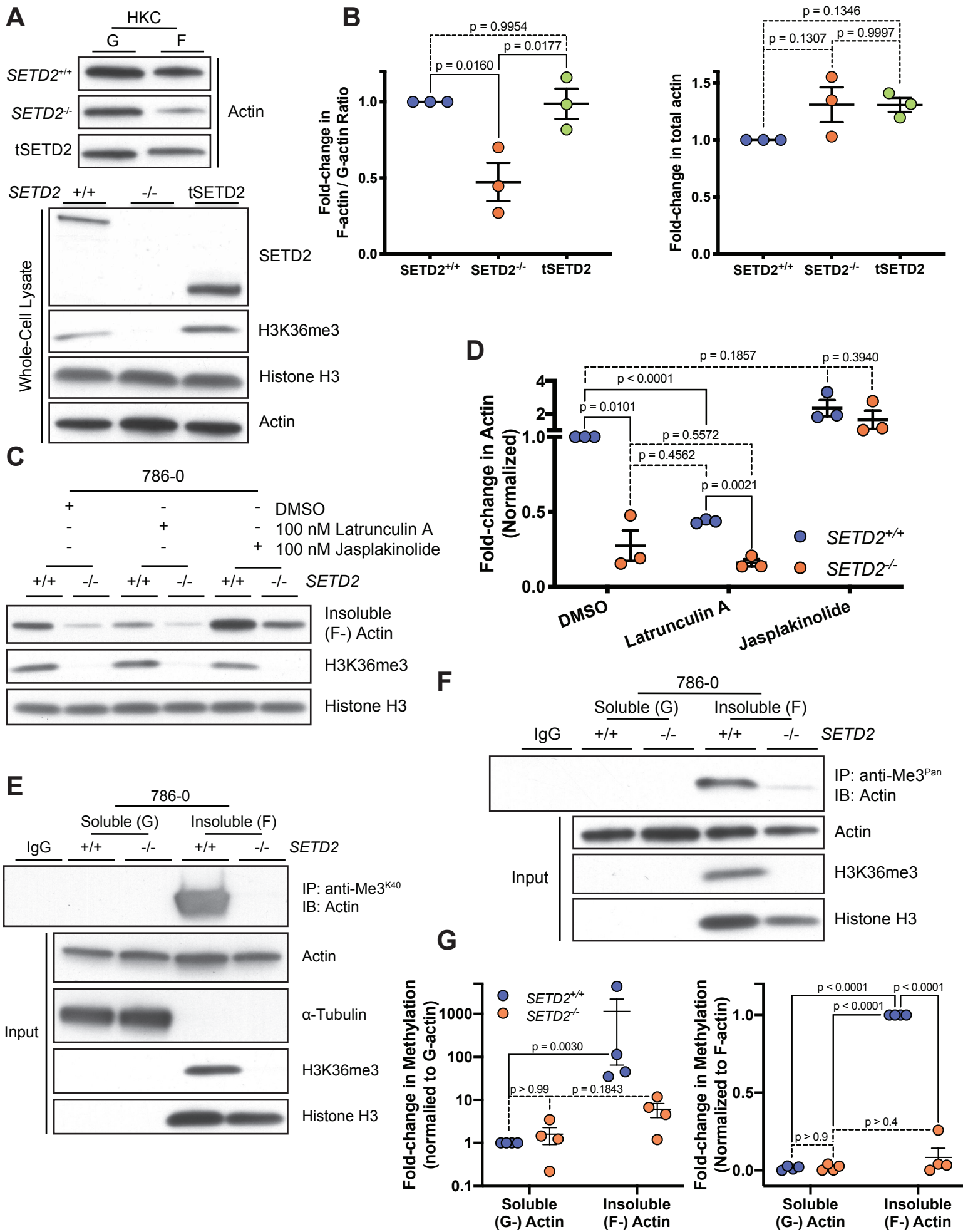
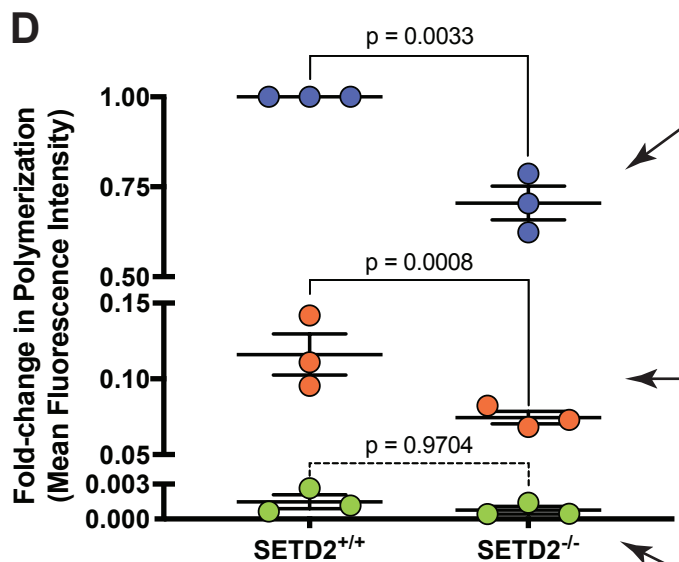
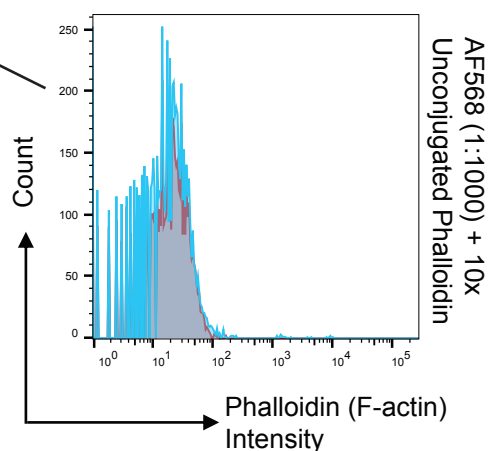
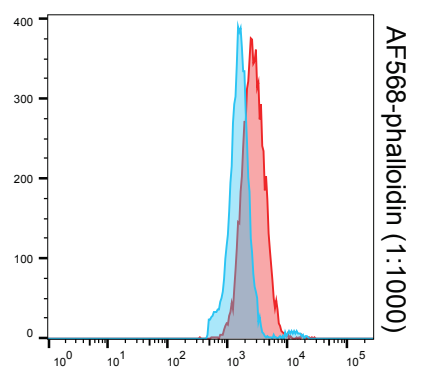
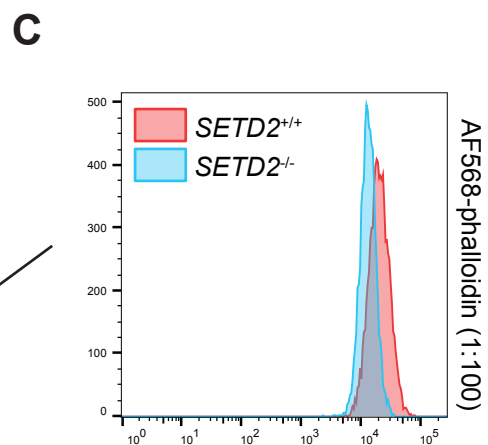
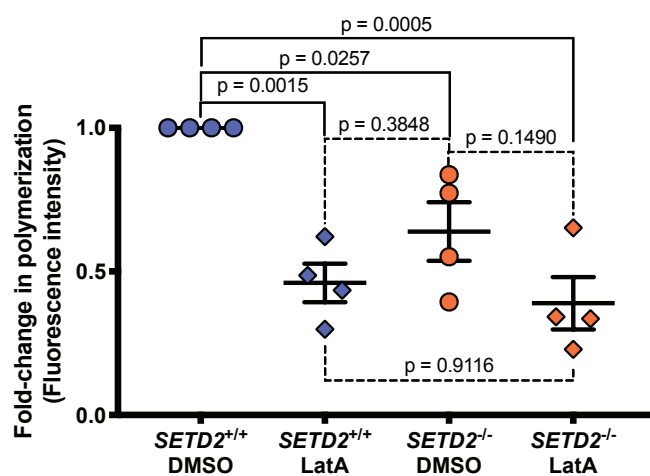
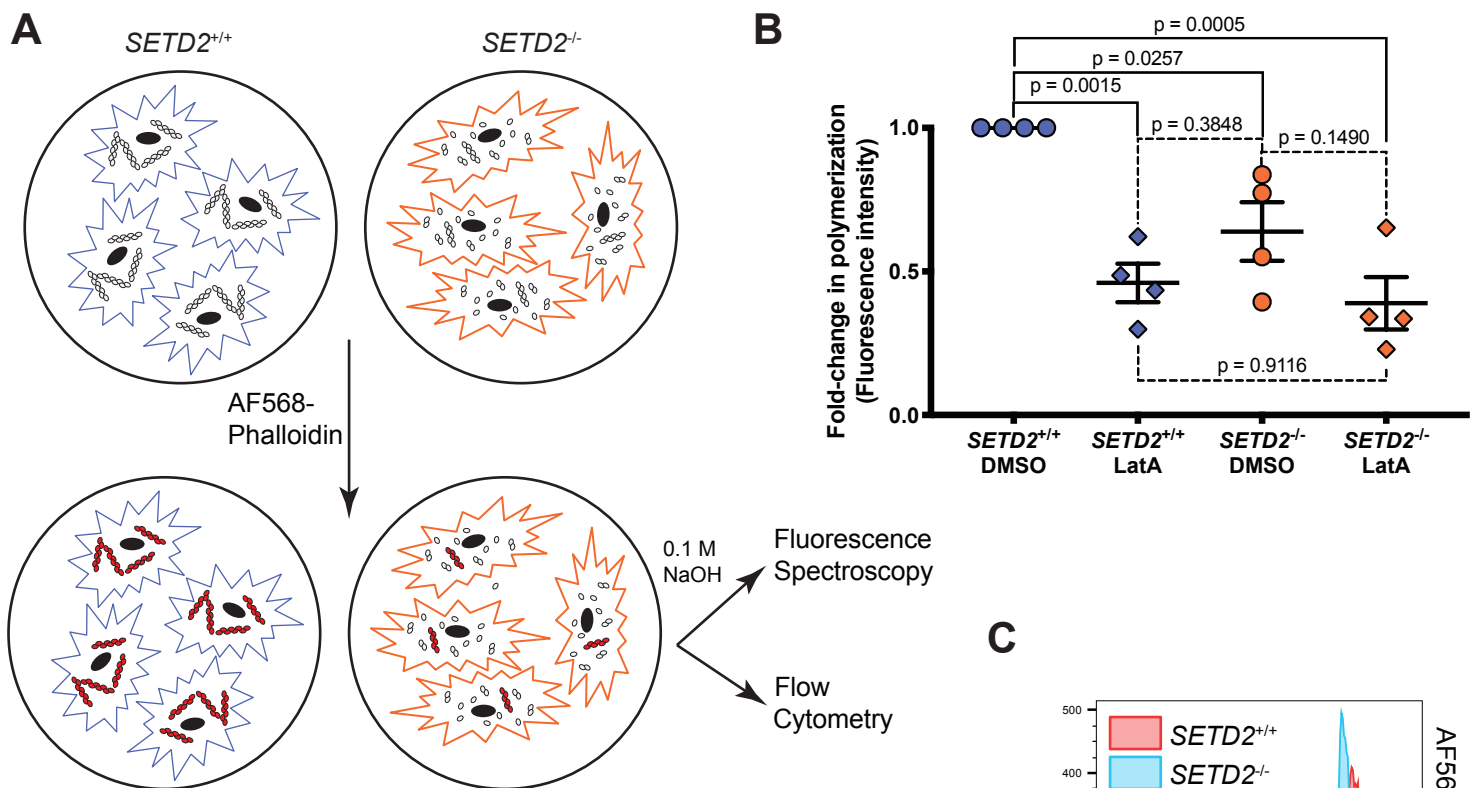


Figure S5. Biochemical evidence for actin defect in SETD2-deficient cells. (A and B) Immunoblot analysis (A) and quantitation (B) showing decreased F-/G- actin ratio in SETD2-deficient HKC cells, rescued with re-expression of truncated SETD2 (tSETD2). Data are mean \pm S.E.M. (n=3). **(C and D)** Immunoblot analysis (C) and quantitation (D) showing changes in insoluble F-actin in 786-0 cells treated with the depolymerizing agent Latrunculin A or the actin polymerizing agent Jasplakinolide. Data are mean \pm S.E.M. (n=3). **(E and F)** Loss of methylation from the polymerized F-actin fraction in SETD2-deficient cells shown by immunoprecipitation of actin from the insoluble fraction of 786-0 cells using SETD2 methyl epitope anti-Me3^{K40} (E) and anti-Me3^{Pan} (F) antibodies. Data shown are representative of experiments repeated four times with similar results. H3K36me3 is used as a control to confirm loss of SETD2 in (C), (E), and (F). **(G)** Quantitation of data shown in (E), normalized to G-actin (left) and F-actin (left), showing a ~100- to 1000:1 ratio of methylated actin in the F-actin versus G-actin fractions. Data are mean \pm S.E.M. (n=4). Quantitation representative of experiments performed with anti-Me3^{K68} and anti-Me3^{Pan} antibodies.



- AF568-Phalloidin (1:100)
- AF568-Phalloidin (1:1000)
- AF568-Phalloidin (1:1000) + 10x unconjugated phalloidin

Figure S6. Actin polymerization defect in SETD2-deficient cells. (A) Schematic drawing of experiments using fluorescent phalloidin to assess polymerized F-actin content in SETD2-proficient versus deficient cells. (B) Quantitation of spectrophotometric analysis of extracted fluorescent phalloidin from 786-0 cells treated with DMSO control or 100 nM Latrunculin A (LatA). Data are mean \pm S.E.M. (n=4). (C) Flow cytometry plots showing intensity of fluorescent phalloidin in SETD2-proficient (red) and SETD2-deficient (blue) 786-0 cell populations. Data are shown for two concentrations of Alexa Fluor 568 (AF568) conjugated phalloidin (1:100, 1:1000), as well as for samples treated with AF568 phalloidin (1:1000) and 10x unconjugated phalloidin as a control. (D) Quantitation of mean fluorescence intensity from (C), with arrows indicating data from each phalloidin concentration. Y-axis split to reflect magnitude of change in phalloidin intensity between SETD2 -proficient and -deficient cells at the three different concentrations: 1:100 (blue) 1:1000 (orange), and 1:1000 + 10x unconjugated (green). Data are mean \pm S.E.M. (n=3).

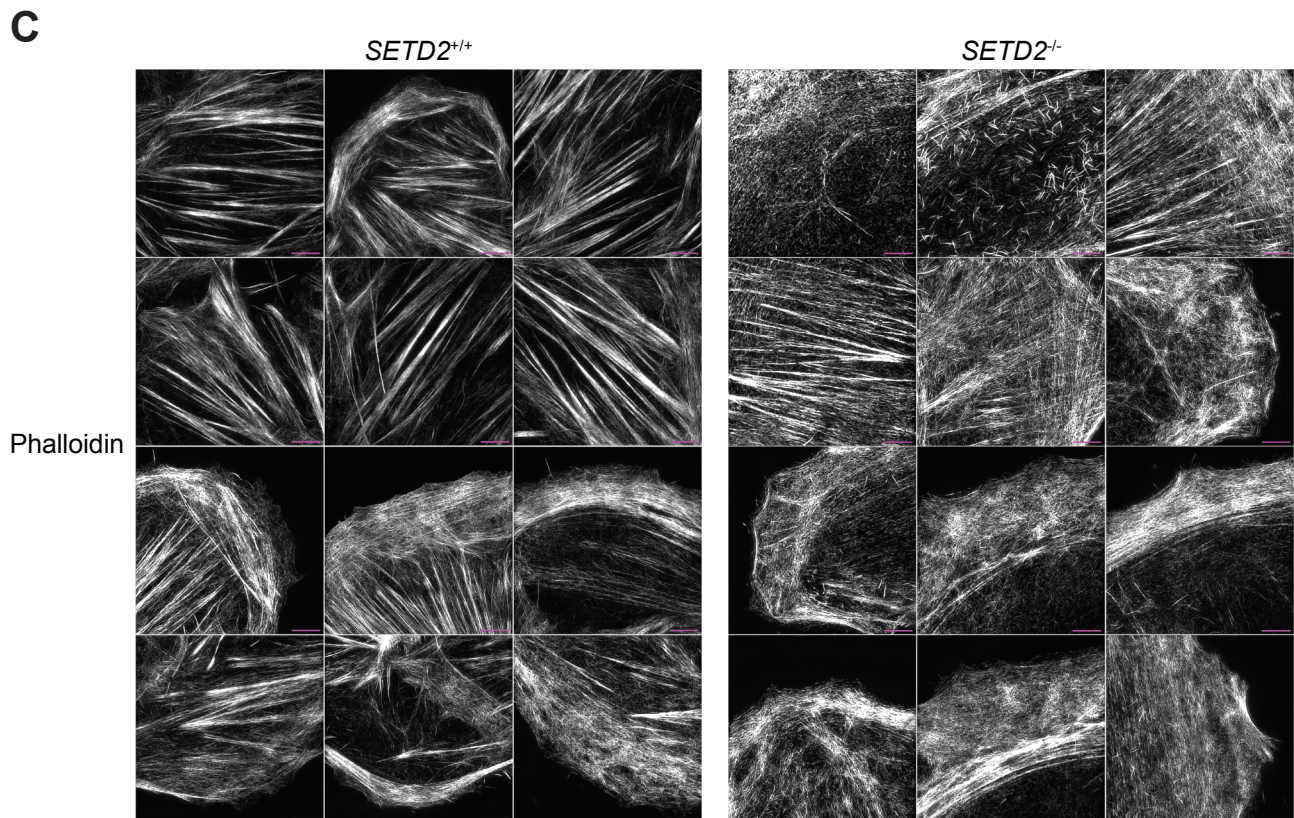
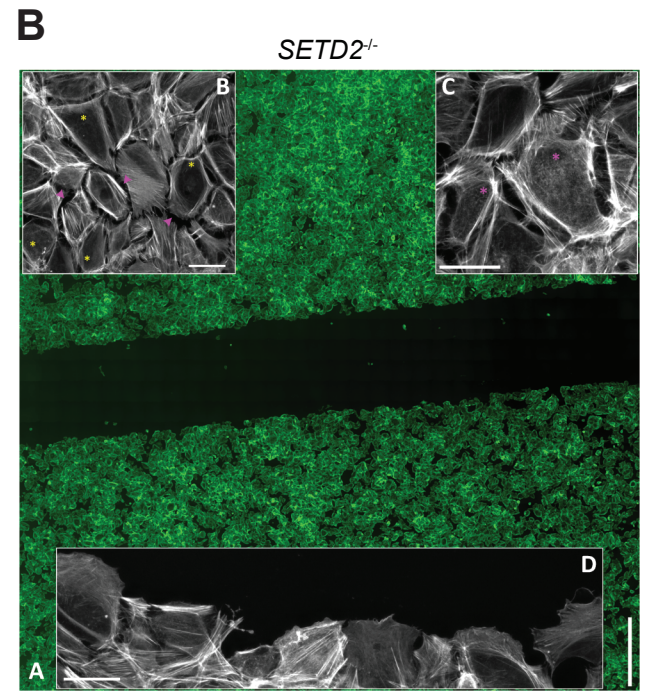
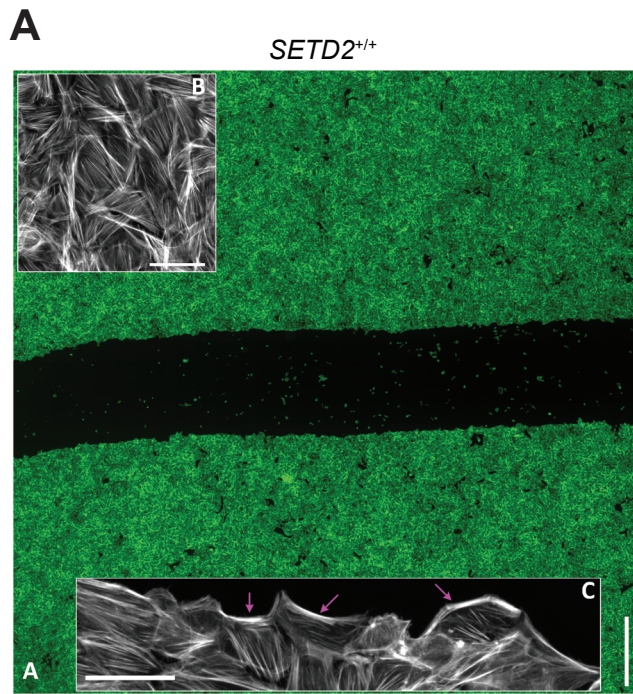


Figure S7. High/Super-Resolution imaging of actin. (A) High-Resolution image stitching of SETD2-proficient HKC cells. Sub-panel A shows the ultra-large field-of-view afforded by this automated imaging approach (Scale bar, 1000 μm). Sub-panel B displays actual resolution of sub-panel A, to reveal highly confluent, tightly packed monolayer of cells, suggestive of robust cell-cell adhesion (Scale bar, 50 μm). Sub-panel C shows retrograde actin arcs (purple arrows) in leading-edge cells (Scale bar, 50 μm). (B) High-resolution imaging of SETD2-deficient HKC cells. Sub-panel A shows ultra-large field-of-view of all cells (Scale bar, 1000 μm). Sub-panel B shows dissolution of cell-cell contacts, as seen by increased pericellular space (purple arrowheads), and reduced stress fibers (yellow asterisks) in these cells (Scale bar, 50 μm). Sub-panel C shows apical actin-based protrusions suggestive of microvilli (purple asterisks) not observed in wild-type populations (Scale bar, 50 μm). Sub-panel D shows lack of robust actin arcs seen in wild-type cells, extended lamella, and cells lacking distinct actin signatures at the leading edge (Scale bar, 50 μm). (C) Super-Resolution imaging (3D-structured illumination microscopy) revealing robust stress fibers in SETD2-proficient cells (left), relative to the highly disorganized meshwork of actin representative of SETD2-deficient cells, along with appearance of microvilli in cells amongst the population (right). Scale bars, 5 μm .

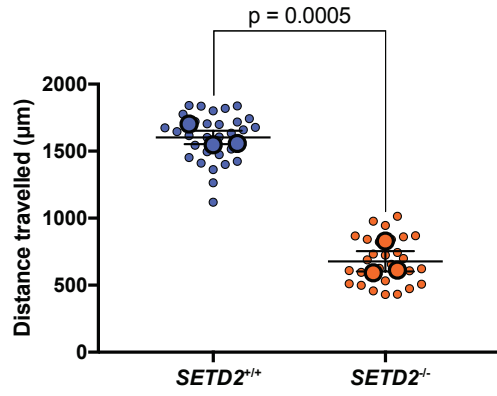
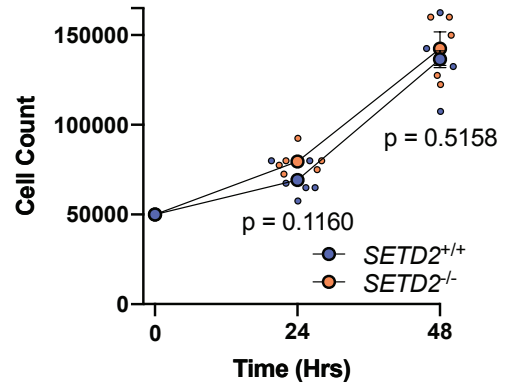
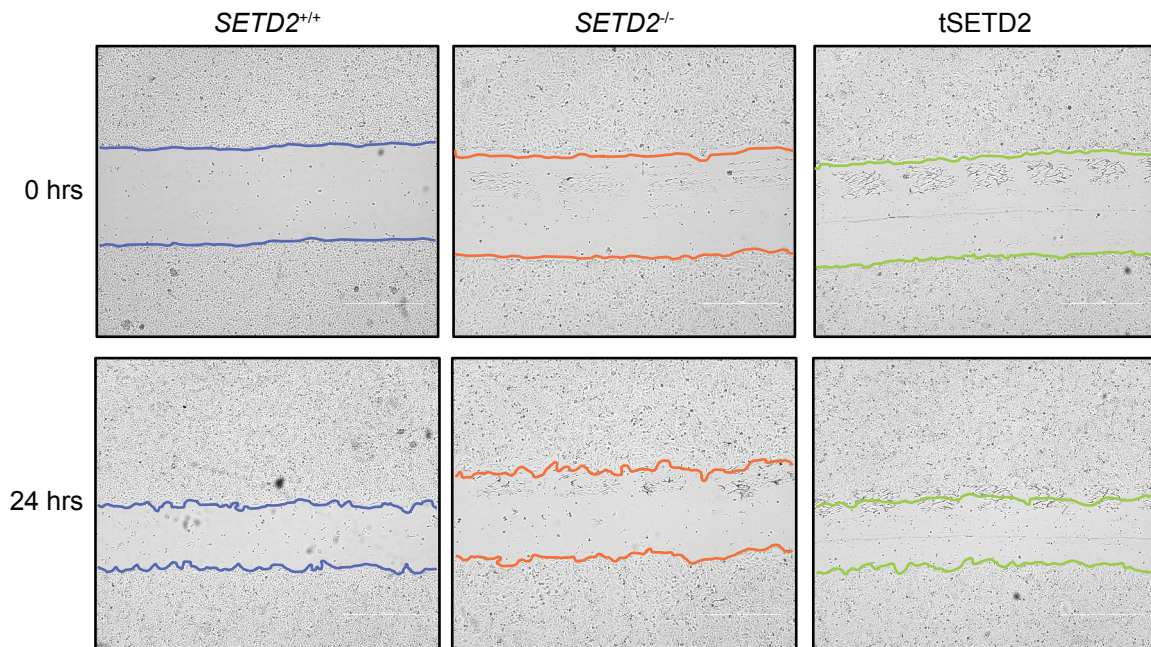
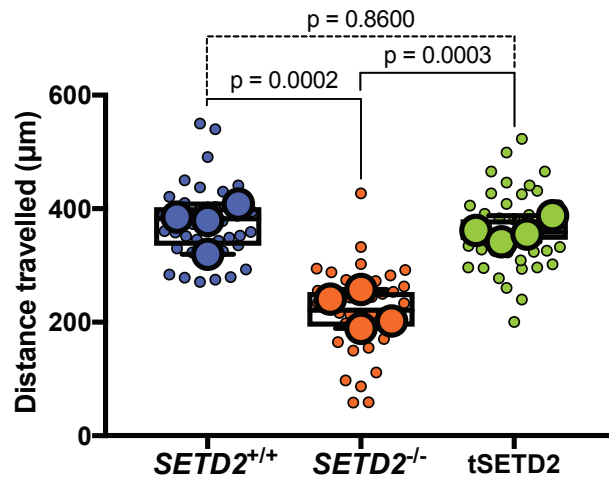
A**B****C****D**

Fig. S8. Proliferation-independent migration defect in SETD2-deficient cells. (A) Quantitation of scratch assay in 786-0 cells treated with cell proliferation inhibitor cytosine arabinoside (AraC). Small circles represent each independent measurement and large circles represent mean from 10 measurements from each independent biological replicate (n=3). **(B)** Cell counts for 786-0 cells over 48 hours (duration of the scratch assay from plating to final measurements). Small circles represent each independent measurement; large circles with error bars are mean \pm S.E.M. for each independent biological replicate (n=2). **(C)** *In vitro* scratch assay at 0 and 24 hours after wound inflection illustrating decreased cell migration in SETD2-deficient versus SETD2-proficient HKC cells, and rescue of defect by re-expression of truncated SETD2 (tSETD2). Scale bars, 1000 μ m. **(D)** Quantitation of data shown in (C). Small circles represent each independent measurement and large circles represent mean from a minimum of 9 measurements for each independent biological replicate (n=4).

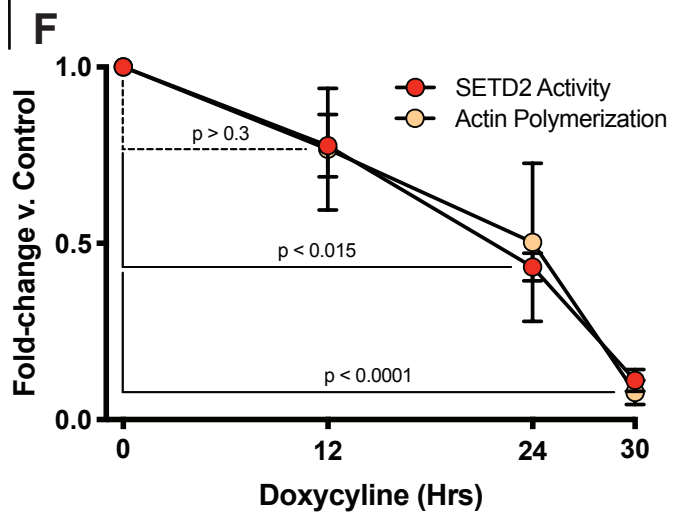
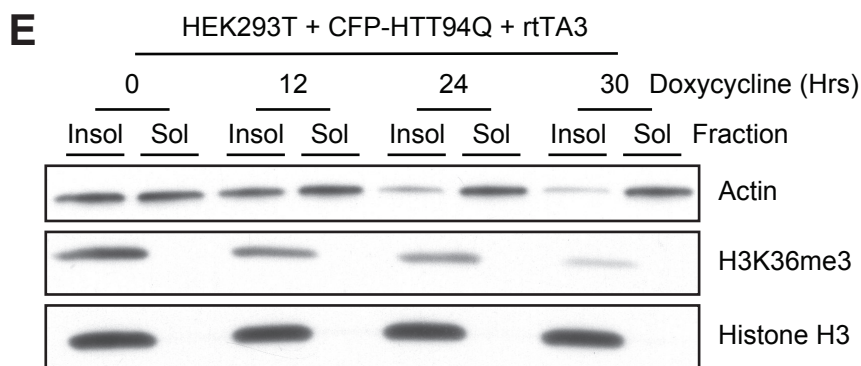
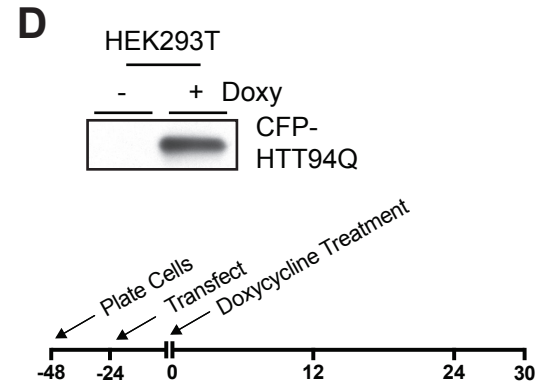
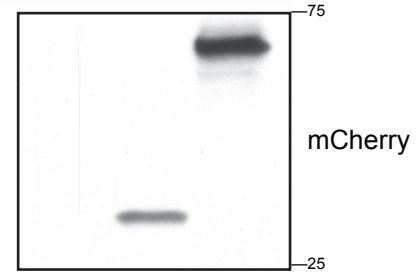
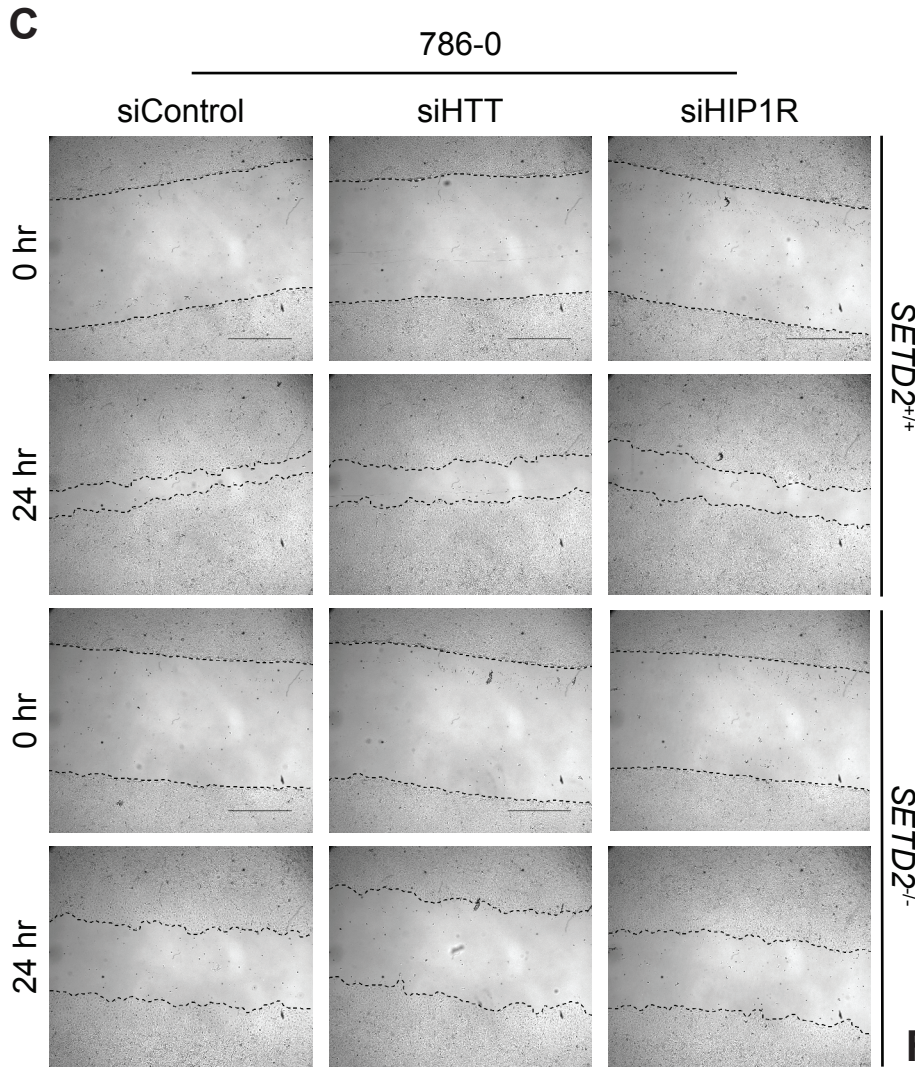
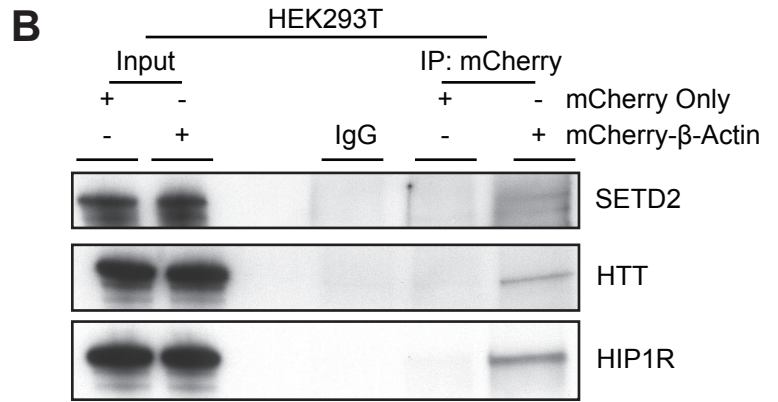
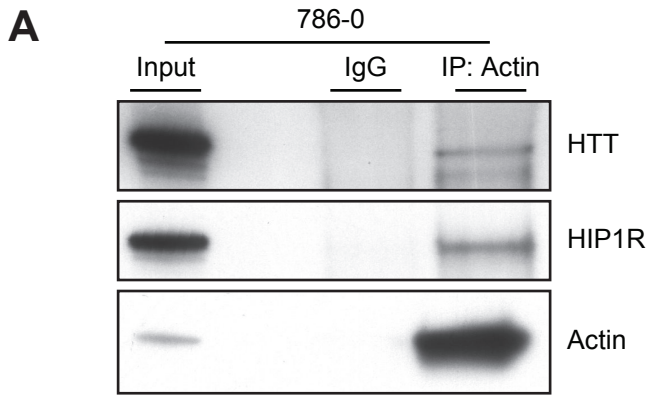


Fig. S9. SETD2-HTT-HIP1R actin methylation axis. (A and B) Immunoblot analysis showing co-immunoprecipitation of endogenous Huntingtin (HTT) and HIP1R with endogenous actin in 786-0 cells (A), and mCherry- β -actin expressed in HEK293T cells (B). Data shown are representative of experiments repeated three times with similar results. (C) *In vitro* scratch assay at 0 and 24 hours after wound inflection illustrating defects in cell migration in SETD2-proficient 786-0 cells after siRNA-mediated knockdown of *HTT* or *HIP1R*. Scale bars, 1000 μ m. Quantitation shown in Fig. 7F. (D) Schematic drawing showing timeline for doxycycline treatment and expression of inducible CFP-tagged N-terminal mutant HTT construct (CFP-HTT94Q) in HEK293T cells. Inlay, immunoblot analysis showing expression of the mutant HTT construct after doxycycline (Doxy) treatment. (E and F) Immunoblot analysis (E) and quantitation (F) showing decrease in ratio of insoluble F-actin to soluble G-actin with expression of CFP-HTT94Q in SETD2-proficient HEK293T cells. H3K36me3 used as a control to assess SETD2 methylation activity in HEK293T cells expressing CFP-HTT94Q. Data are mean \pm S.E.M. (n=3).

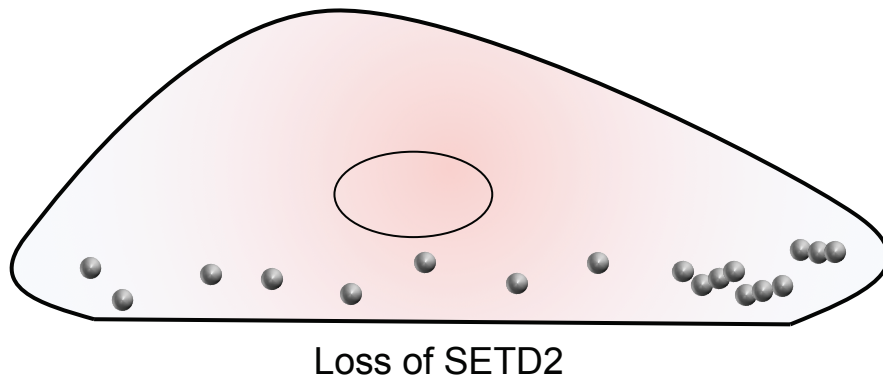
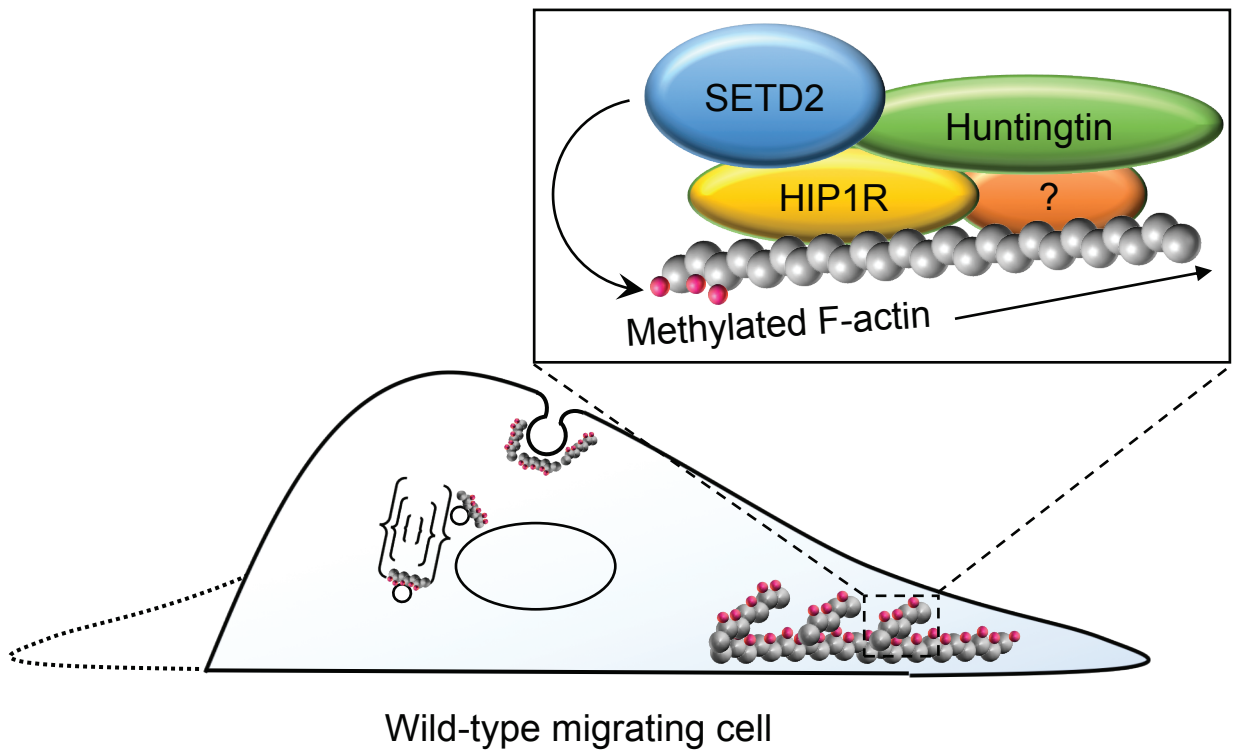


Fig. S10. Model of the SETD2-HTT-HIP1R axis for actin lysine methylation. Schematic diagram showing SETD2 methylates actin in a cellular complex containing the scaffolding protein huntingtin and the actin-binding adapter HIP1R. SETD2 methylation is required for normal cellular actin dynamics; loss of SETD2 negatively impacts actin dynamics and cell migration.

Supplemental Movies S1-S3. 3-dimensional rendering of cells shown in Figure S7. Movie S1 shows robust stress fibers in SETD2-proficient cells, which are less frequent and disorganized in SETD2-deficient cells (Movie S2). Additionally, while microvilli can be found in SETD2-proficient cells, they are found more frequently and appear more robust in SETD2-deficient populations (Movie S3).